MSW MANAGEMENT -Multidisciplinary, Scientific Work and Management Journal
ISSN: 1053-7899
Vol. 36 Issue 1, 2026, Pages 6504-6512

The impact of particle contamination on Functionally Graded Material based Spacer for GIS applications

Nallagatla Vasundhara[1,a] and Venkata Nagesh Kumar Gundavarapu[2,b*]
[1] Lecturer in EEE, Government Polytechnic for Women, Kadapa, Research Scholar JNTUAnanthapuramu, Anantapur District, Andhra Pradesh, India.
[2]Professor, Department of EEE, JNTUA College of Engineering Kalikiri, Andhra Pradesh, India.
[a]n.vasu74@gmail.com, [b]drgvnk14@gmail.com

Abstract- Electrical substations must operate safely, effectively, and promptly following damage. Recent problems with the insulator surface of GIB, including delamination and protrusion, have resulted in de-energization of the device and substantial financial losses. A three-phase GIB exhibiting delamination, voids, protrusions, depressions, and particle contamination is built utilizing a delta-type Functionally Graded Material (FGM) spacer to facilitate the examination of electric field stress at the Triple Junction. Metal inserts placed at the enclosure's terminus mitigate electrical stress. Distributed FGM, infused with varying permittivity values and diverse filler materials, yields a uniform electrical field stress. Variations in GIB and FGM voltage ratings are utilized in the simulation. The incorporation of the metal insert into the FGM insulator significantly mitigates the impact of grading on electric field stress, as previously established.

Key Words-Field Stress, Triple Junction, Gas Insulated Busduct, FGM, Green Gas and MetalInsert.

1. INTRODUCTION

Now-a-days, a reliable electrical supply cannot be guaranteed without the continuous functioning of substations. The existing air-insulated substations are unable to achieve this due to recurrent shutdowns resulting from energy loss. Due to its compact size, high density, and low maintenance needs, Gas Insulated Systems (GIS) are employed in numerous electrical and industrial applications. GIS is employed in High Voltage Substations, Transmission Lines, Industrial Facilities, Wind Farms, Transportation Infrastructure, Utilities, Specialized Environments (such as Mining Operations and Chemical Plants), Emergency and Critical Facilities, and Renewable Energy Integration. Their application improves the reliability, security, and durability of electrical systems in several industries.
Theoretically, the exclusive remedy to address the current problem with the existing substations is to deploy gas-insulated substations, which enclose the entire transmission system within a chamber filled with dielectric gas to reduce energy loss and guarantee stable, reliable electricity. Concurrently with the rapid increase in urbanization and energy use, the GIB is presently experiencing more attraction. These problems must be resolved to enhance the return on investment for gas-insulated switchgear at the substation. Therefore, they must address the environmental impacts of their operations while simultaneously reducing costs, improving dependability, and preserving operational flexibility.

Numerous studies on spacers have demonstrated that GIB spacer faults deteriorate insulation over time. G.V. Nagesh Kumar et al. [1] identified that particles are generated either during the operation of circuit breakers or during the manufacturing process. Due to their ability to move freely or remain stationary on the spacer surface, free conducting particles have been demonstrated to be the most hazardous in GIBs. Based on their composition, these particles may function as insulators or conductors. Insulating particles, conversely, have less impact on spacers. Numerous further researchers [2-8] have observed that particles are confined within the enclosure's surface. The erratic motion of particles near coaxial conductors is influenced by the angle of incidence and the coefficient of restitution. Researchers have utilized approaches such as dielectric coating to reduce the effects of contaminated particles in GIB. A unique approach utilizing a metal insert has been developed to further mitigate the impact of particles. Muneaki et al. [9] investigated the implementation of the FGM technique to improve the compactness of GIS and reduce electric stress. An analysis of the fundamental epoxy spacer was performed utilizing the Finite Element Method (FEM), taking into account various permittivity values. The research by Maren Istad et al. [10] indicates that the existence of loose and mobile particles in SF6 gas causes flashovers in the GIB, resulting in considerable energy loss and more flashovers. Numerous defects, such as loose metallic particles, particles on the spacer, and delamination, have been identified by several authors [11-14]. The dimensions, shape, positioning, and contamination of metallic particles adjacent to the spacers are criteria that influence the emergence of these defects during production. This results in a partial release of the electric field. Qikun Feng et al. [15] examined the impact of depression on insulators at extensive distances. Electric stress exceeded that in supported enclosed structures, even within highly conductive materials.

A study by Feng Chang Gu et al. [16] discovered different irregularities in the internal conductors of porcelain bushings on the gearbox line. The anomalies were classified as follows: Category 1 pertains to the conductivity of porcelain hollow cylindrical bushings filled with oil lubricant; Category 2 relates to gas tanks that generally contain metallic particulates; Category 3 addresses the operational management of the bushings affected by metalworking depression. M. Thomas.G et al. [17] applied a thin dielectric coating to the inner conductor of GIS to ensure the safe and reliable functioning of the GIB amidst particulate contamination within the spacer. According to study by Purnomoadi et al. [18], electric field distributions in GIS might manifest as homogeneous, quasi-homogeneous, or inhomogeneous. Affixing the particle to the epoxy material adjacent to the electrode produces an inhomogeneous field configuration, hence resulting in a significantly amplified electric field at the particle's extremities. Minimizing the impact of metal particles on pressurized Gas Insulated Substations enhances their reliability. One proposed method involves the application of adhesive coatings to GIB electrodes.

This research analyzes the stress in a three-phase GIB incorporating a functionally graded material delta spacer under various anomalies, including voids, delaminations, protrusions, and particle contamination. Metal-insulators are integrated at the zero potential terminal to reduce electric stress at junctions and maintain a consistent surface field. The recessed metal component safeguarded the triple connection, diminishing TJ Estress. This MI methodology made insulator replacement more economical and efficient. The stress distribution at the thermal junction of the functionally graded material spacer was assessed after the completion of the necessary replicas.

2. MODELING OF THREEPHASE GIB

Using the Laplace and Poisson equations' boundary conditions, researchers have computed the E_{stress}. Since it is thought to be challenging to compute analytically, these equations are employed to determine "E_{stress}." Complex problems are solved using the FEM, despite the availability of multiple numerical techniques.

Equation (1) expresses electric flux density ($\vec{D}$) as E_{stress}($\vec{E}$)

$$\vec{D} = \varepsilon \vec{E} \tag{1}$$

Equation (2) describes the electric fluxDensity D with Qi as electrical charge on a closed surface.

$$\oint_S \vec{D} \bullet \vec{dS} = Q_i \tag{2}$$

E → is defined by equation (3). The equation (3) gives the relationship b/w electric field intensity and electric potential in three dimensions, which will be substituted into the point form of the first equation, div D =row v, to get a final voltage expression, del square V= zero.

$$\vec{E} = -\left(\vec{a_x}\frac{\partial}{\partial x} + \vec{a_y}\frac{\partial}{\partial y} + \vec{a_z}\frac{\partial}{\partial z}\right)V \tag{3}$$

Equation (4) gives Estressin its x,y co-ordinates.

$$\vec{E} = \vec{a_x}\frac{\partial V(x,y)}{\partial x} - \vec{a_y}\frac{\partial V(x,y)}{\partial y} \tag{4}$$

A/c to divergence theorem,

$$\left(\vec{a_x}\frac{\partial}{\partial x} + \vec{a_y}\frac{\partial}{\partial y} + \vec{a_z}\frac{\partial}{\partial z}\right) \bullet \left(\vec{a_x}\frac{\partial D_x}{\partial x} + \vec{a_y}\frac{\partial D_y}{\partial y} + \vec{a_z}\frac{\partial D_z}{\partial z}\right) = \rho_v \tag{5}$$

when dielectric materials are homogenous, linear

$$\Gamma V = \frac{-\rho_v}{\varepsilon} \quad \text{Where} \quad \Gamma = \frac{\partial^2}{\partial x^2} + \frac{\partial^2}{\partial y^2} + \frac{\partial^2}{\partial z^2} \tag{6}$$

Uniform charge distribution reduces volume charge density, simplifying equation (6) to eqn(7).

$$\Gamma V = 0 \tag{7}$$

MSW MANAGEMENT -Multidisciplinary, Scientific Work and Management Journal
ISSN: 1053-7899
Vol. 36 Issue 1, 2026, Pages 6504-6512

Figure 1 illustrates the typical delta-shaped spacer. The flux densities on both sides should be constant.

The complete volume 'v' of the area under consideration stores W of electrical energy. $W = \frac{1}{2}\int\int\int \varepsilon\left(\nabla^2 V\right)dv$

(8)

then,

$$dW = \frac{1}{2}\int\int \varepsilon\left(\nabla^2 V\right)dxdy = 0 \quad (10)$$

As $\nabla^2 V = 0$, from equation (10)

$$dW = 0 \quad (11)$$

3. A FUNCTIONALLY GRADED MATERIAL DELTA SPACER WITH PARTICLE

Delta-spacers are among the most basic insulators utilized in Gas Insulated Busbars (GIB) relative to other insulators. This spacer is positioned perpendicularly b/w the conductor and the enclosure end. During flashovers, the electric field distribution may be non-uniform due to the greater permitivity of the spacer material compared to the surrounding gas. The permittivity of the spacer is redistributed within the medium utilizing the FGM approach to diminish the intensity of the electric field at the surface interface. The delta-shaped FGM spacer consists of seven consistent gradations across all three spacers according to their lengths. The impact of FGM gradings is assessed using GL, GH, and GU within the permittivity spectrum.

Figure 1 illustrates the depiction of the delta spacer composed of GREEN GAS under particle contamination, an environmentally sustainable insulating material utilized in GasInsulated Substations.

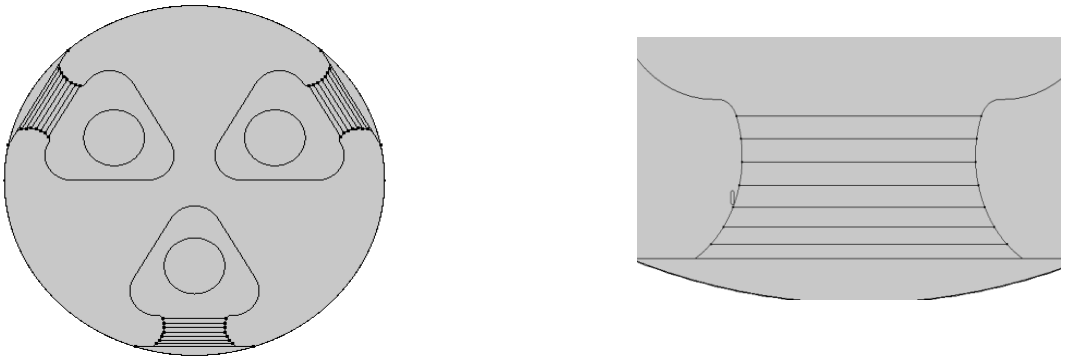

Fig.1. delta spacer without MI UNDER PARTICLE

The spacer is circular and features three triangular parts placed in a delta configuration. Each segment contains a central aperture designed to accommodate a conductor. This design maintains uniform spacing of the wires, offers structural support, and mitigates electrical issues like as flashovers. The utilization of GREEN GAS renders the spacer environmentally benign while maintaining excellent electrical and mechanical performance

TABLE-1.Electric fieldIntensity of delta spacer without MI under particle contamination

CONDUCTOR'	72.5 KV stress at enclosure KV/cm	220 KV stress at enclosure KV/cm	765 KV stress at enclosure KV/cm
R	0.0493	01497	0.3681
Y	0.0280	0.0850	0.2090
B	0.0269	0.0817	0.2010

Figure 2 illustrates the representation of the delta spacer with a METAL INSERT (MI). Simulations are conducted using delta-spacers for various voltages.

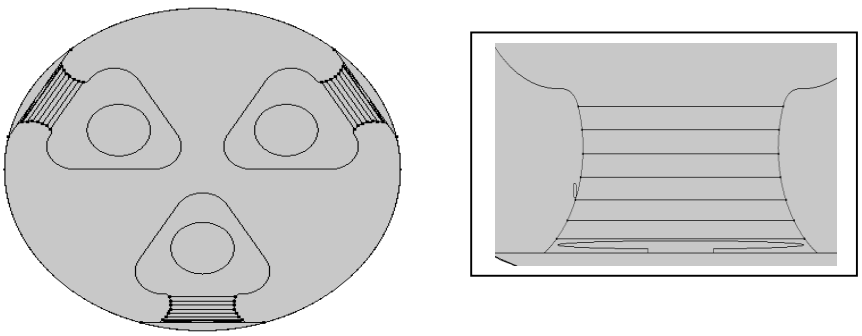

Fig.2.depiction of delta spacer withMI under particle

TABLE-2.Electric field intencity of delta spacer with Metalinsert under particle contamination

CONDUCTOR	72.5 KV fieldstress at enclosure KV/cm	220 KV fieldstress at enclosure KV/cm	765 KV fieldstress at enclosure KV/cm
R	0.0320	0.0970	0.2386
Y	0.0161	0.0489	0.1202
B	0.0157	0.0475	0.1169

The assessment of Tables 1 and 2 indicates a notable decrease in electric field intensity at the enclosure when a metallic insert is included in the delta-spacer. The electric field stress for the R-phase conductor diminished by roughly 24.65% across all voltage levels: 72.5 kV, 220 kV, and 765 kV. Conversely, the Y and B-phase

MSW MANAGEMENT -Multidisciplinary, Scientific Work and Management Journal
ISSN: 1053-7899
Vol. 36 Issue 1, 2026, Pages 6504-6512

conductors demonstrated a more significant decline, with stress values decreasing by around 39% at each voltage level. The continuous decrease demonstrates that incorporating a metal insert in the spacer design significantly mitigates electric field stress, especially for the Y and B conductors. This lowering enhances the dielectric performance and reliability of the GIS system by minimizing the danger of insulation failure caused by high electric stress concentrations. Figures 1 and 2 illustrate the design of the delta spacer structure both with and without a metal insert (MI), particularly in the presence of a defect particle, which demonstrates notable variations in electric field behavior and stress distribution. In the design devoid of a metal insert, the electric field lines exhibit a greater concentration around the defect particle owing to the discontinuity in permittivity. The lack of a conductive insert results in less directed pathways, leading to localized stress concentrations around the particle. This can markedly elevate the danger of insulation breakdown, particularly at elevated voltage levels. It mitigates the detrimental impacts of defect particles, resulting in reduced electric field stress levels and enhanced performance at high voltage settings.

3.1 VOID WITH PARTICLE

The illustrations presented illustrate a delta-spacer utilized in GIS, notably emphasizing the existence of defects such as particles and vacancies. Figure 3 distinctly illustrates the configuration of the voids, depicted by several horizontal lines interspersed inside the spacer material. In comparison to an impeccable delta spacer design, which ensures uniform electric field distribution and enhanced insulation dependability, the flawed design presented here underscores the significant influence of even little defects. The existence of particles and voids markedly undermines the efficacy and dependability of the insulating system in GIS, highlighting the necessity for meticulous manufacture and stringent quality control.

Fig.3.Zoomed Design of delta spacer with particle &Void

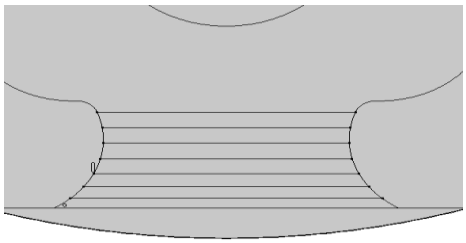

Fig.4. Design of delta spacer with Particle & Void with MI

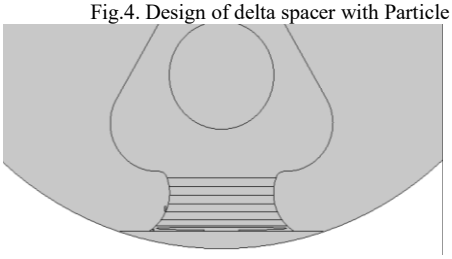

Figure 4 illustrates the structural design of the delta-spacer, which incorporates both voids and particles, as well as a metal insert (MI). This setup is more intricate than the spacer without MI. The existence of gaps and particles within the material might disrupt the electric field distribution, while the metal insert contributes to further field augmentation along its edges owing to its high conductivity.

3.2 DELAMINATION WITH PARTICLE

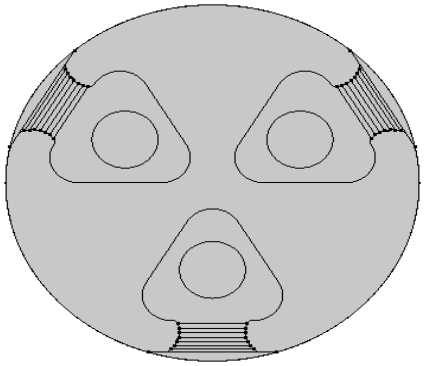

Fig.5. Design of delta spacer with delamination with particle

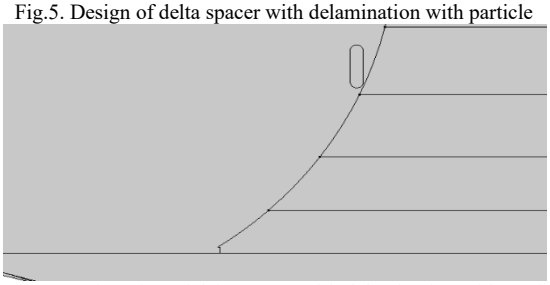

Fig.6 Zoomed Design of delta spacer with delamination with particle

Figures 5 and 6 depict the design of a delta-spacer featuring particle and delamination, absent a metal insert. Figure 5 illustrates the entire delta spacer structure, featuring a minor delaminated area (gap or fracture) positioned near the spacer's surface. The lack of a metal insert streamlines the internal structure; yet, the presence of particles and delamination remains a concern. These faults can disrupt the electric field and may result in partial discharge or insulation failure over time. Figure 6 illustrates an enlarged depiction of the delaminated region. The separation between material layers is distinctly observable. Particles confined in delaminated regions may serve as loci of electrical stress concentration. In the absence of a metal insert, the spacer depends entirely on the insulating material; thus, any imperfections such as delamination become significantly more critical and can adversely impact performance.

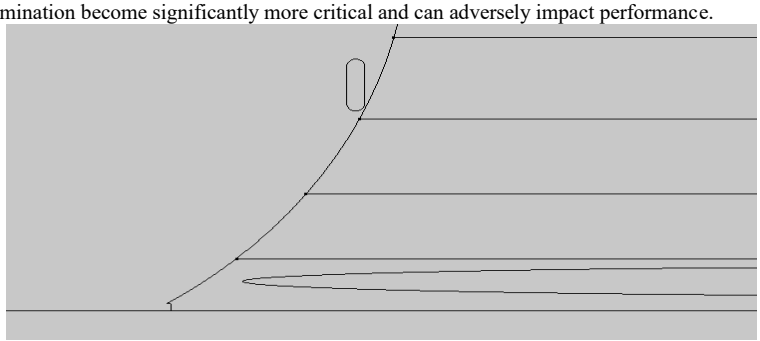

Fig.7. Zoomed Design of delta spacer with Particle & delamination with MI

MSW MANAGEMENT -Multidisciplinary, Scientific Work and Management Journal
ISSN: 1053-7899
Vol. 36 Issue 1, 2026, Pages 6504-6512

The design of the delta-spacer, seen in Figure 7, emphasizes critical structural attributes and potential failure causes, including particle inclusion and delamination. The spacer contains a metallic inlay, presumably designed to augment its mechanical strength or performance. The magnified perspective discloses a foreign particle embedded within the material layers, potentially introduced during the manufacturing process. Such particles can compromise the material's integrity, serving as loci of weakness and precipitating fractures. Moreover, delamination is identified as a split between material layers, signifying inadequate adhesion or stress-related degradation. This spacing can markedly diminish the strength and durability of the spacer. The interplay of the particle, delamination, and the interface with the metal insert illustrates how various factors can converge and result in structural deterioration if inadequately managed during the design and production phases.

3.3 PROTRUSION WITH PARTICLE

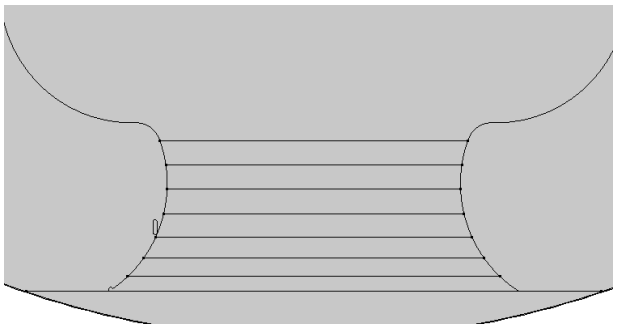

Fig.8 Zoomed Design of delta spacer with Protrusion & Particle

The Delta Spacer with Protrusion and Particle, depicted in Fig. 8, features a circular cross-section with three symmetrical triangular (delta-shaped) cut-outs that serve as the primary functional geometry for electric field regulation in a high-voltage setting. Each delta cavity contains a central circular vacuum, potentially signifying the site of electric field intensification or insulation interface zones. The existence of protrusions (presumably elevated features on the inner surface) and particles (possibly impurities or dielectric debris) within the spacer can interfere with the uniform distribution of the electric field. These faults may result in partial discharges, surface tracking, or insulation deterioration under elevated voltage stress.

The illustrations depict the configuration of a delta-spacer featuring a metallic insert, alongside observable imperfections including protrusions and particles. Figure 9 presents a top view of the spacer, which exhibits a circular arrangement with three symmetrically positioned delta-shaped cavities. At the center of each hollow, a round region is evident, maybe indicating the placement of the metal inserts.

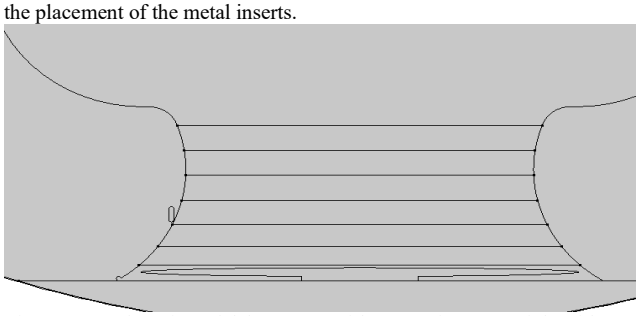

Fig.9. Zoomed Design of delta spacer with Protrusion & Particle with MI

These inserts are generally incorporated to augment mechanical strength, improve wear resistance, or ensure solid anchoring for interconnected components. Nonetheless, these regions also exhibit indications of irregularities—potentially manifesting as protrusions or embedded particles—which may influence the quality and performance of the component.

4. RESULTS AND DISCUSSIONS

The delta-type spacer without a metal insert results in increased electric field intensity at the triple junctions (TJ) of conductors A, B, and C, indicating poor field control. A detailed evaluation of electric field stress at the enclosure for different Functionally Graded Materials (LG-FGM, HG-FGM, and UG-FGM) across voltage levels of 72.5 kV (V1), 220 kV (V2), and 765 kV (V3) shows that stress consistently increases with voltage for all phases (R, Y, B) and configurations (C-1, C-2, C-3). In LG-FGM, the Red phase records the highest stress, reaching 0.3681 kV/cm at 765 kV, while Yellow and Blue phases show lower values (~0.2090 kV/cm and ~0.2010 kV/cm). The reduction from configuration C-1 to C-3 is minimal, contributing to only about 2–3% decrease in electric field stress, indicating limited effectiveness of configuration changes alone.

In HG-FGM, the electric field stress is slightly higher than LG-FGM, with the Red phase peaking at 0.3897 kV/cm, which is approximately 5.86% higher than LG-FGM, indicating increased stress concentration. Similarly, the Yellow and Blue phases also show higher values, suggesting that HG-FGM intensifies the electric field rather than reducing it. On the other hand, UG-FGM demonstrates intermediate behavior, with a maximum stress of 0.3706 kV/cm, which is about 4.90% lower than HG-FGM but slightly higher than LG-FGM (~0.68% increase). Overall, UG-FGM provides a balanced performance with improved uniformity. Thus, without a metal insert, the spacer exhibits higher electric field stress, with only 2–3% reduction due to configuration changes, while material grading influences stress levels by up to 5–6% variation, highlighting the necessity of incorporating a metal insert for effective stress reduction.

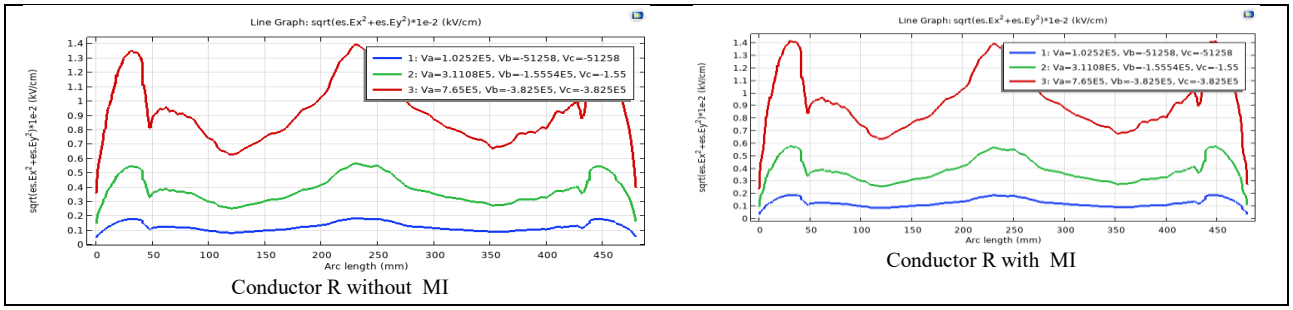

Conductor R without MI

Conductor R with MI

MSW MANAGEMENT -Multidisciplinary, Scientific Work and Management Journal
ISSN: 1053-7899
Vol. 36 Issue 1, 2026, Pages 6504-6512

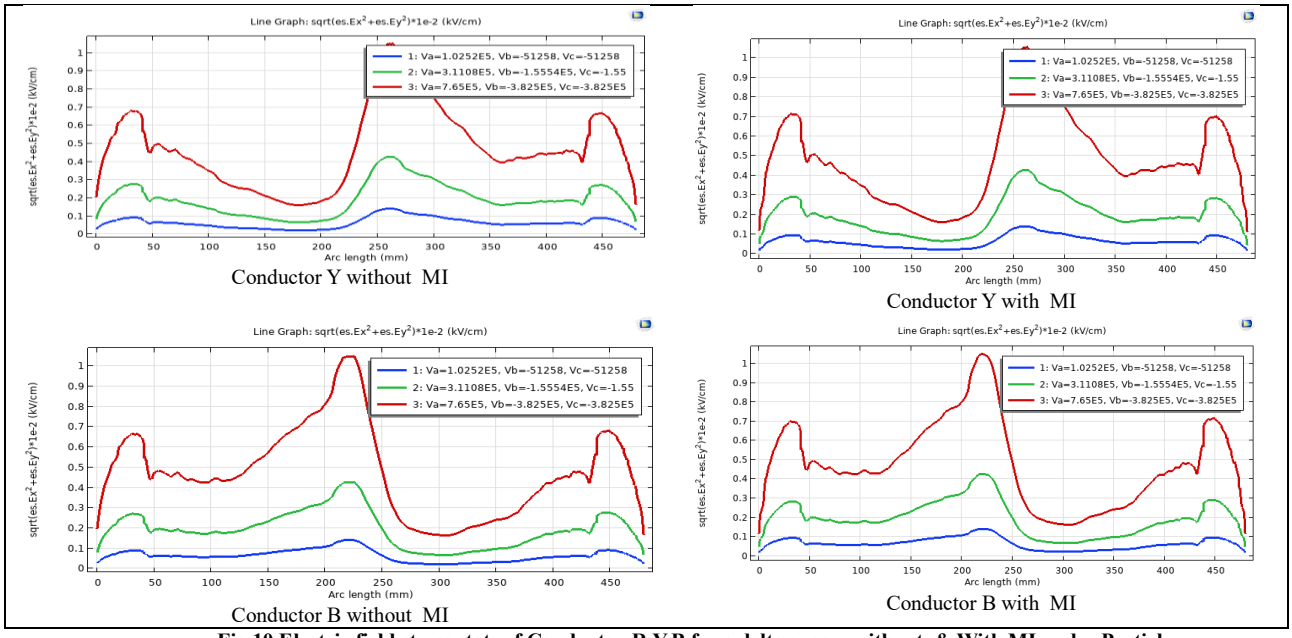

Fig 10 Electric field stress stats of Conductor-R,Y,B for a delta spacer without & With MI under Particle

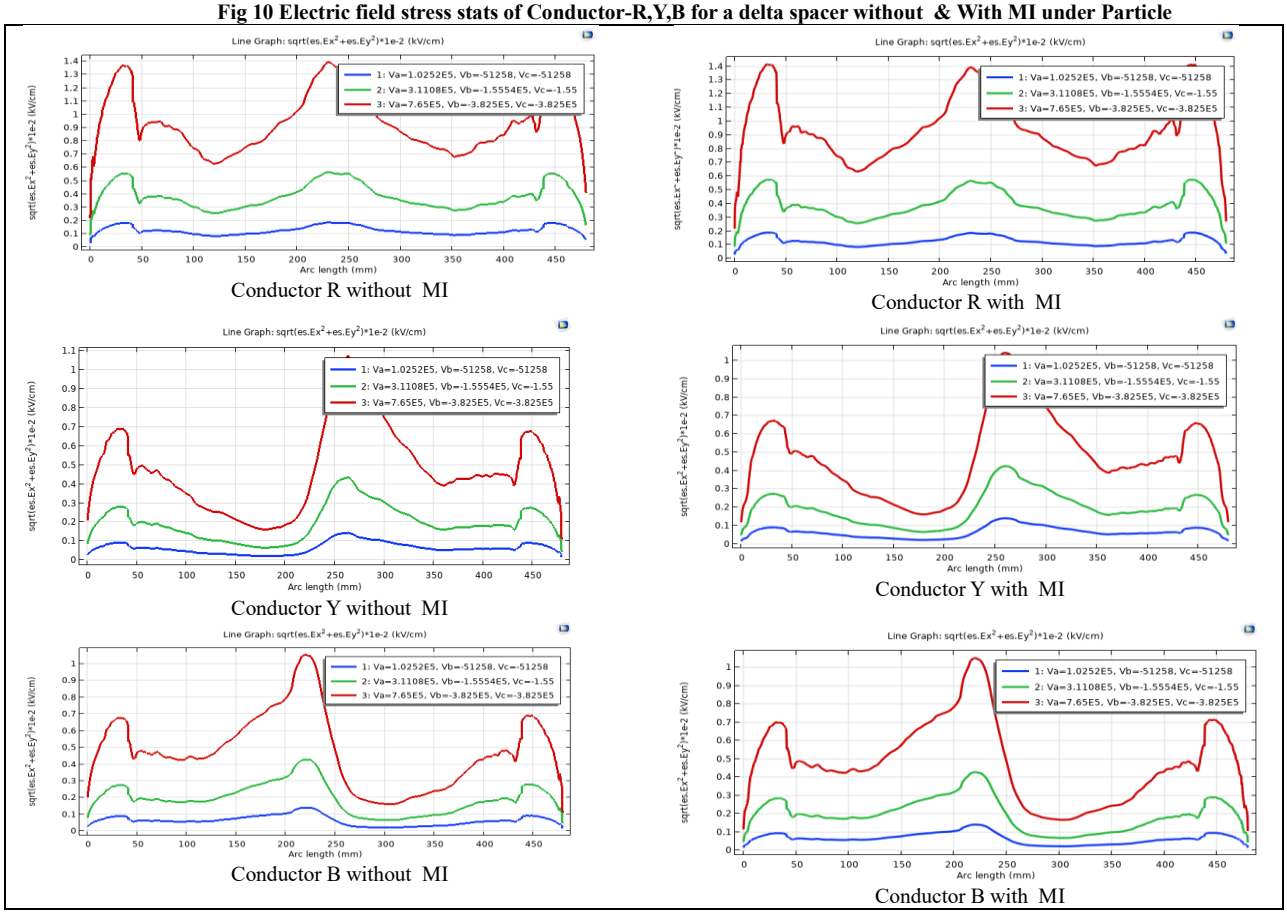

Fig 11 Electric field stress of Conductor-R,Y,B for a delta spacer without & With MI under particle with Void defect

An analogous electric stress of 0.0254 kV/cm at V1, 0.0782 kV/cm at V2, and 0.1923 kV/cm at V3 is noted at the enclosure end of conductor-Y, as seen in the figure. The graph indicates that at varying operating voltages V1, V2, and V3, the electric stress at the enclosure end of conductor-B measures 0.0248 kV/cm, 0.0752 kV/cm, and 0.1849 kV/cm, respectively.

MSW MANAGEMENT -Multidisciplinary, Scientific Work and Management Journal
ISSN: 1053-7899
Vol. 36 Issue 1, 2026, Pages 6504-6512

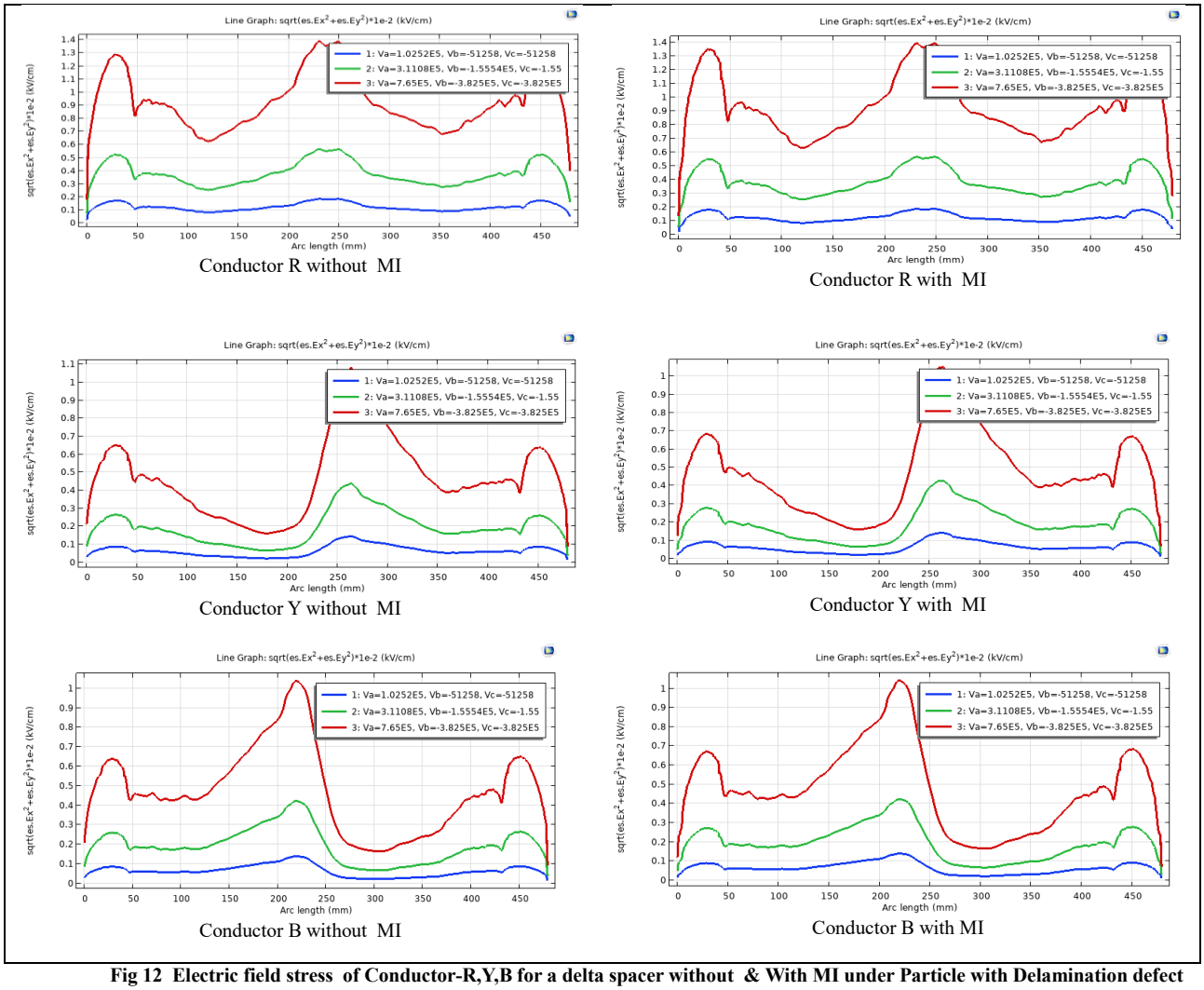

Fig 12 Electric field stress of Conductor-R,Y,B for a delta spacer without & With MI under Particle with Delamination defect

To mitigate the failure of three-phase GIB, it is essential to employ a suitable strategy to reduce the field stress generated at the terminal junction of all three conductors. A suitably sized and shaped metal insert placed into the enclosing end of each of the three spacers will do this. Data from the tables indicate that the field stress at the enclosure ends of all conductors decreases to the required level after the introduction of metal inserts; however, there is no observable reduction at the conductor ends of spacers due to the presence of metal inserts at those locations.

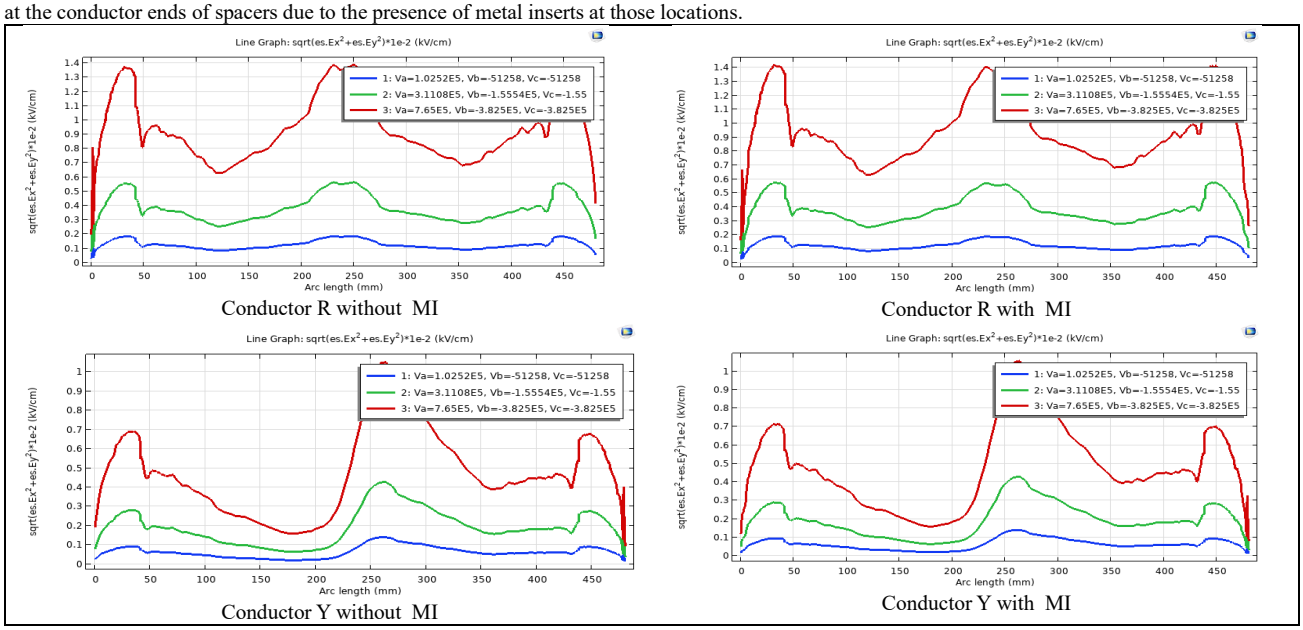

MSW MANAGEMENT -Multidisciplinary, Scientific Work and Management Journal
ISSN: 1053-7899
Vol. 36 Issue 1, 2026, Pages 6504-6512

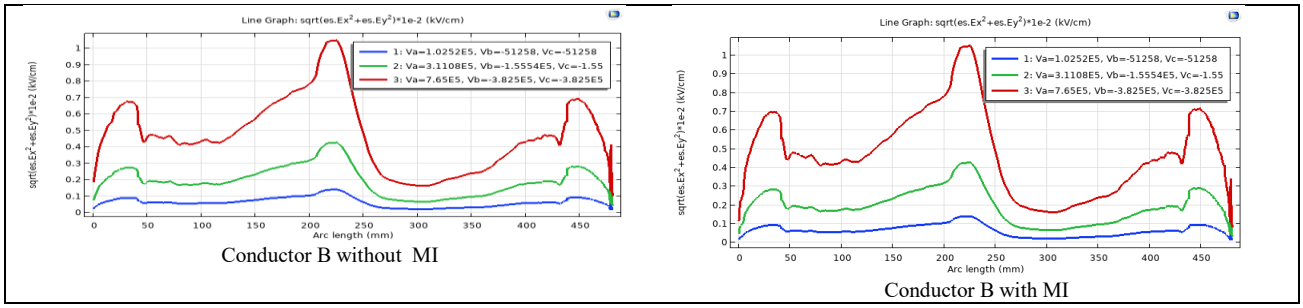

Fig 13 Electric field stress of Conductor-R,Y,B for a delta spacer without & With MI under Particle with Protrusion defect

TABLE 3. Comparative analysis of Estress for 765 kV, LG-FGM grading

Electric field stress at 765kV LG-FGM Grading at enclosure end under various abnormalities along with particle							
		Without MI	With MI	Without MI	With MI	Without MI	With MI
conductor	Permittivity	Protrusion with particle		Void with particle		Delamination with particle	
R	C_1	0.1974	0.1609	0.2288	0.2213	0.1598	0.1181
	C_2	0.1929	0.1573	0.2258	0.2184	0.1557	0.1150
	C_3	0.1885	0.1538	0.2230	0.2155	0.1519	0.1120
Y	C_1	0.1918	0.1202	0.2079	0.1208	0.2084	0.1210
	C_2	0.1899	0.1191	0.2058	0.1196	0.2064	0.1199
	C_3	0.1881	0.1180	0.2038	0.1185	0.2044	0.1188
B	C_1	0.1846	0.1166	0.2018	0.1152	0.2016	0.1155
	C_2	0.1828	0.1155	0.1998	0.1141	0.1996	0.1144
	C_3	0.1811	0.1145	0.1979	0.1131	0.1977	0.1134

TABLE 4. Comparative analysis of Estress for 765 kV, HG-FGM grading

Electric field stress at 765kV HG-FGM Grading at enclosure end under various abnormalities							
		Without MI	With MI	Without MI	With MI	Without MI	With MI
conductor	Permittivity	Protrusion with particle		Void with particle		Delamination with particle	
R	C_1	0.2215	0.1777	0.2444	0.2339	0.1824	0.1330
	C_2	0.2158	0.1732	0.2406	0.2302	0.1772	0.1291
	C_3	0.2103	0.1689	0.2371	0.2267	0.1723	0.1254
Y	C_1	0.2011	0.1244	0.2183	0.1250	0.2187	0.1252
	C_2	0.1988	0.1231	0.2158	0.1236	0.2162	0.1239
	C_3	0.1967	0.1218	0.2134	0.1223	0.2138	0.1226
B	C_1	0.1935	0.1208	0.2121	0.1194	0.2118	0.1197
	C_2	0.1914	0.1195	0.2096	0.1181	0.2093	0.1184
	C_3	0.1893	0.1182	0.2073	0.1168	0.2070	0.1171

TABLE 5. Comparative analysis of Estress for 765 kV, UG-FGM grading

Electric field stress at 765kV HG-FGM Grading at enclosure end under various abnormalities							
		Without MI	With MI	Without MI	With MI	Without MI	With MI
conductor	Permittivity	Protrusion with particle		Void with particle		Delamination with particle	
R	C_1	0.1988	0.1620	0.2303	0.2228	0.1610	0.1189
	C_2	0.1940	0.1581	0.2272	0.2195	0.1568	0.1156
	C_3	0.1896	0.1545	0.2243	0.2166	0.1529	0.1126
Y	C_1	0.1931	0.1210	0.2092	0.1215	0.2098	0.1218
	C_2	0.1910	0.1197	0.2070	0.1202	0.2076	0.1205
	C_3	0.1892	0.1185	0.2049	0.1191	0.2055	0.1193
B	C_1	0.1859	0.1174	0.2032	0.1160	0.2030	0.1163
	C_2	0.1840	0.1161	0.2010	0.1147	0.2008	0.1150
	C_3	0.1822	0.1150	0.1990	0.1136	0.1989	0.1139

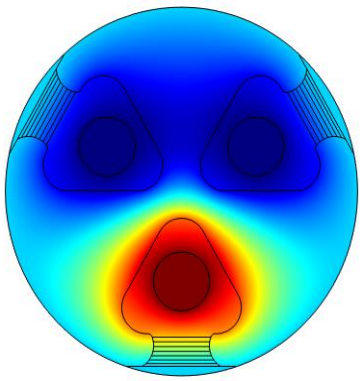

Fig.14.Surface plot of a spacer of the delta type without MI

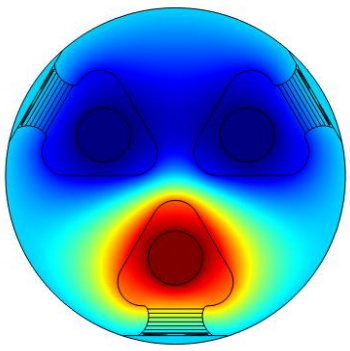

Fig.15. Surface plot of a spacer of the cylindrical type with MI

MSW MANAGEMENT -Multidisciplinary, Scientific Work and Management Journal
ISSN: 1053-7899
Vol. 36 Issue 1, 2026, Pages 6504-6512

conductor	Permittivity	Without MI	With MI	Without MI	With MI	Without MI	With MI
		Protrusion		Void		Delamination	
R	C-1	0.2126	0.1948	0.2280	0.2135	0.2086	0.1935
	C-2	0.2871	0.1907	0.2031	0.2010	0.3871	0.2060
	C-3	0.2452	0.1179	0.2718	0.2444	0.2452	0.2444
Y	C-1	0.2241	0.248	0.240	0.2066	0.2940	0.2766
	C-2	0.2363	0.1252	0.2165	0.2084	0.2663	0.2584
	C-3	0.2938	0.1753	0.2942	0.1807	0.2938	0.2807
B	C-1	0.2829	0.2093	0.2106	0.1535	0.2906	0.2735
	C-2	0.2652	0.1898	0.2013	0.1973	0.2952	0.2873
	C-3	0.2754	0.2297	0.1356	0.1222	0.2554	0.2422

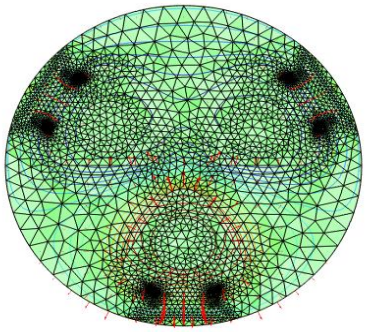

Fig.16. MeshPlot of Delta Spacer without MI

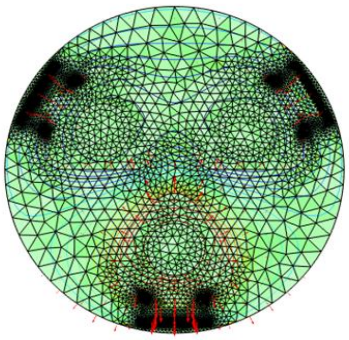

Fig.17. MeshPlot of Delta Spacer with MI

conductor	Permittivity	Without MI	With MI	Without MI	With MI	Without MI	With MI
		Protrusion		Void		Delamination	
R	C-1	0.1994	0.1590	0.2200	0.2179	0.1696	0.1183
	C-2	0.1948	0.1554	0.2171	0.2150	0.1654	0.1151
	C-3	0.1904	0.1519	0.2143	0.2122	0.1613	0.1121
Y	C-1	0.1927	0.1202	0.2080	0.1204	0.2086	0.1193
	C-2	0.1909	0.1191	0.2059	0.1193	0.2065	0.1182
	C-3	0.1891	0.1180	0.2039	0.1182	0.2046	0.1171
B	C-1	0.1869	0.1155	0.2006	0.1150	0.2016	0.1160
	C-2	0.1851	0.1144	0.1986	0.1139	0.1996	0.1149
	C-3	0.1834	0.1133	0.1967	0.1128	0.1977	0.1138

TABLE 6. Analysis of E_{stress} for 765 kV, LG-FGM grading for Bulb Type Spacer

Tables 7 shows the results of the proposed delta type spacer which is designed and the results are presented. A comparative analysis of the Table 6 and 7 shows how the present design achieves superior electric field mitigation, reduced stress concentrations, and potential reliability benefits compared to conventional spacer designs reported in prior studies.Figures 14 and 15 depict the field distribution of the delta-type through two surface plots. Figure 13 illustrates the delta spacer devoid of a metal insert (MI), whereas Figure 15 presents the delta spacer with a metal insert. In contrast, Fig. 15 illustrates that the delta spacer with MI exhibits a more uniform and smoother field distribution. The red zones exhibit reduced intensity and improved confinement, indicating that the field stress is more efficiently controlled with the inclusion of a metal insert. The seamless gradient transition from red to blue in this plot indicates less peak stress and enhanced dielectric performance.Figures 16 and 17 depict the finite element discretization of the delta spacer, both without and with the metal insert (MI), respectively. These visualizations are essential for comprehending the model's segmentation into discrete components for numerical simulations, including electric field stress analysis. In Fig. 16, the mesh of the delta spacer devoid of MI exhibits a rougher and more uneven texture in the area of elevated field concentration, particularly around the lower center where denser red vectors, signifying a higher electric field gradient, are observed. Conversely, Fig. 17—the mesh plot of the delta spacer with MI—exhibits a significantly finer and more uniform mesh distribution in the important areas, especially adjacent to the center region and the electrodes.

5. CONCLUSIONS

The analysis of the delta-type spacer without a metal insert clearly indicates poor electric field control, with significant stress concentration at the triple junctions of all three conductors. The electric field stress increases with voltage across all configurations and material gradings, showing that higher operating conditions further aggravate insulation stress and reduce system reliability. Among the materials, LG-FGM exhibits comparatively lower stress, while HG-FGM shows higher stress concentration, and UG-FGM provides a more balanced and uniform field distribution. However, the variation due to material grading is limited, and configuration changes alone offer only minimal improvement in reducing electric field stress. Overall, the results confirm that without a metal insert, the spacer cannot effectively control electric field intensity. Therefore, the incorporation of a metal insert becomes essential to achieve significant stress reduction, improved field uniformity, and enhanced reliability of the GIB system.

- The protrusion effect leads to elevated stress values in all conductors R, Y, and B across all operating voltages among the various anomalies. The comparison analysis concludes that protrusion is the most severe consequence among all anomalies.
- In instances of delamination accompanied by particles, the electric field stress reaches its maximum at the site of delamination and the particle in the LG-FGM case-3 grading, while the minimum field stress occurs in the HG-FGM case-1 grading across all conductors for the various operating voltages examined. The electric field stress at the particle's position exceeds that at the delamination site.
- In the case of voids and particles, the largest electric field stress is observed at the locations of both voids and particles under HG-FGM case-1 grading, while electric stress is diminished under UG-FGM case-3 grading throughout all three conductors for various operating voltages. The electric field stress at the particle's location exceeds that at the void's place.
- Comparatively, the most severe field stresses were detected in instances of delamination involving particles rather than voids in the presence of particles. The resultant stress due to delamination and voids caused by particles has been reduced through the incorporation of a recessed metal insert at the transition joint of the zero potential end.
- This investigation indicates that the use of a metal insert diminishes the elevated field stresses caused by delamination defects and particles, achieving lower values in the UG-FGM case-2 grading across all conductors R, Y, and B for all working voltages.

MSW MANAGEMENT -Multidisciplinary, Scientific Work and Management Journal
ISSN: 1053-7899
Vol. 36 Issue 1, 2026, Pages 6504-6512

In all operating voltages, LG-FGM case-1 Gradings exhibit the most significant reduction in Estress at the void and particle locations, attributable to the combined effects of the void and particle.

- In all instances of LG, HG, and UG-FGM gradings, the maximum percentage reduction in Estressis observed at TJ of zero potential end was derived from the analysis of FGM Bulb spacers with delamination and particle defects.
- The proposed FGM delta-spacer technique offers an improved solution for the distribution of the electric field along the spacer's surface. Additionally, the incorporation of a metal insert at the enclosure end of the spacer effectively reduces the enhanced electric field intensities at the sites of delamination, voids, and particles across all conductors. In future work, experimental validation and prototype testing will be conducted to further corroborate the simulation results and assess the practical performance of the proposed design.

References

[1] G.V. Nagesh Kumar, J. Amarnath, B.P. Singh, K.D. Srivastava, "Electric Field Effect on Metallic Particle Contamination in a Common Enclosure Gas Insulated Busduct" , IEEE Transactions on Dielectrics and Electrical Insulation,Vol. 14(2), pp.334-340,2007.

[2] G. V. Nagesh Kumar, J. Amarnath, B.P.Singh, "Motion of Free Conducting Particles in a Single Phase Compressed Gas Insulated Busduct with Electromagnetic Field Effect", IEEE International Conference on Condition Monitoring and Diagnosis, CMD 2008.

[3] M.Venu Gopala Rao, G.V.Nagesh Kumar, J.Amarnath, S.Kamakshaiah, "Effect of Various Design Parameters on the Movement of Metallic Particles in a Three Phase Common Enclosure Gas Insulated Busduct", IEEE Conference on Electrical Insulation Dielectric Phenomena, pp.367-370,2008.

[4] D.Padmavathi, G.V. Nagesh Kumar, J.Amarnath, D. Deepak Chowdary, "Dielectric Behavior of Compact Design Three Phase Coated Gas Insulated Busduct with Metallic Particle Contamination", IEEE International Conference on High Voltage Engineering and Application , pp. 399-403, 2008.

[5] M.Ramya Priya, G.V.Nagesh Kumar, J.Amarnath and R.Prabha Devi, "Effect of Various Design Parameters of Gas Insulated Bus Duct in the Performance of Gas Insulated Sub-Stations", IEEE International Conference on Control Automation Communication and Energy Conservation , pp. 1-4, 2009.

[6] G.V. Nagesh Kumar, J. Amarnath, B.P. Singh , K.D. Srivastava, "Particle initiated discharges in gas insulated substations by random movement of particles in electromagnetic fields", International Journal of Applied Electromagnetics and Mechanics ,Vol.29 ,pp.117–129,2009.

[7] G V Nagesh Kumar, J Amarnath, B P Singh, D Deepak Chowdary, "Influence of unbalanced voltages on the movement of metallic particle in a three phase common enclosure gas insulated busduct" , Journal of Emerging Trends in Engineering and Applied Sciences, Vol. 35(4),pp.393-406,2010.

[8] G.V.N. Kumar, J. Amarnath, B.P. Singh & K.D. Srivastava, "Modelling and Analysis of Metallic Particle Movement in a Common Enclosure GIB With Electromagnetic Field", International Journal of Modelling and Simulation, Vol. 30(1), pp.38-51,2010.

[9] M.Ramya Priya, G.V.Nagesh Kumar, J.Amarnath and R.Prabha Devi, "Effect of Various Design Parameters of Gas Insulated Bus Duct in the Performance of Gas Insulated Sub-Stations", IEEE International Conference on Control Automation Communication and Energy Conservation , pp. 1-4, 2009.

[10] N. Rama Rao, J. Amarnath, "Metallic Particle Trajectory in an Isolated Conductor Gas Insulated Busduct(GIB) With Dielectric Coated Enclosure using Charge Simulation Method", IEEE Conference on Electrical Insulation and Dielectric Phenomena, pp.526-529,2011.

[11] Muneaki. K, Katsumi. K, Masahiro. H, Yoshikazu Hoshina , Masafumi Takei , Hitoshi Okubo, "Application of Functionally Graded Materialfor Reducing Electric Field on Electrode and Spacer Interface", IEEE Transactions on Dielectrics and Electrical Insulation Vol. 17(1), pp.256- 263 ,2010.

[12] Maren Istad , Magne Runde "Thirty-Six Years of Service Experience with a National Population of Gas-Insulated Substations", IEEE Transactions on Power Delivery ,Vol.25(4),pp. 2448 – 2454, 2010.

[13] Genyo Ueta, Junichi Wada, Shigemitsu Okabe, Makoto Miyashita, Chieko Nishida, Mitsuhito Kamei, " Insulation Performance of Three Types of Micro-defects in Inner Epoxy Insulators, IEEE Transactions on Dielectrics and Electrical Insulation", Vol.19(3), pp.947-954,2012.

[14] Wensheng Gao, Dengwei Ding, Weidong Liu, Xinhong Huang "Analysis of the Intrinsic Characteristics of the Partial Discharge Induced by Typical Defects in GIS" IEEE Transactions on Dielectrics and Electrical Insulation, Vol. 20(3), pp.782-790,2013.

[15] Khan.Y, " Partial discharge pattern analysis using PCA and back-propagation artificial neural network for the estimation of size and position of metallic particle adhering to spacer in GIS", Electrical Engineering, Vol. 98 (1), pp. 29-42, 2016.

[16] Moreno.M.V.R, Robles.G, Albarracín.R, Rey.J.A, Tarifa.J.M.M, "Study on the self-integration of a Rogowski coil used in the measurement of partial discharges pulses", Electrical Engineering, Vol.99 (3), pp. 817-826, 2017.

[17] Qikun Feng,Nianqin Dai Beijing, "Analysis And Study On Distribution Of Defect Electric Field On Basin-type Insulator In GIS" ICAEER 2018 .

[18] Feng-Chang Gu, Hung-Cheng Chen, Bo-Yan Chen "A Fractional Fourier Transform-Based Approach for Gas-Insulated Switchgear Partial Discharge Recognition" Journal of Electrical Engineering & Technology, Vol.14, pp. 2073 -2084,2019.

[19] Thomas.G , Davoud.E.M, Joachim Speck, Karsten Backhaus , Tobias Gabler , Steffen G ,Philipp Simka, Uwe Riechert, "Surface discharge behaviour of coated electrodes in gas-insulated systems under DC voltage stress", IEEE Conference on Electrical Insulation and Dielectric Phenomena, pp.477-480, 2018.

[20] A.P. Purnomoadi, A. Rodrigo Mor, J.J. Smit, "Spacer flashover in Gas Insulated Switchgear (GIS) with humid SF6 under different electrical stresses", Electrical Power and Energy Systems- Elsevier, Vol.116 pp. 1-9 , 2020.